Control Coordination Within a VSC HVDC Link for Power Oscillation Damping: A Robust Decentralized Approach Using Homotopy

Yousef Pipelzadeh, *Student Member, IEEE,* Balarko Chaudhuri, *Senior Member, IEEE,* Tim C. Green, *Senior Member, IEEE*

***Abstract*—Power oscillations can be damped effectively through modulation of both active and reactive power of a voltage source converter (VSC) based high voltage direct current (HVDC) link. The challenge, however, is how to coordinate the control action properly at the two ends of the link without using a centralized control scheme which require fast communication of control signals to remote actuator (converters) sites. A full centralized controller may result in a closed-loop performance worse than open-loop in case of a communication loss of feedback signal(s). Alternatively, with block-diagonal control structure, the individual control loops are decoupled from each other which are not only easier to implement in a decentralized way but also shown to guarantee a certain level of performance. Here the concept of homotopy is applied to obtain a single block-diagonal controller from a set of full controllers, individually designed to ensure specified closed-loop performance for a set of operating conditions. Simulation studies in DIgSILENT PowerFactory are carried out on two test systems to demonstrate both robustness and control coordination in a decentralized framework.**

***Index Terms*—HVDC, VSC, Stability, Damping, Decentralized Control, Linear Matrix Inequalities (LMI), Bilinear Matrix Inequalities (BMI), System Identification, Modal Residues, RGA**

I. Introduction

SUPPLEMENTARY modulation of active power through an high voltage direct current (HVDC) link to improve damping of low frequency power oscillations in host AC networks has been exercised by network operators like WECC since the 1970s [1]. With an increasing number of HVDC installations around the world, especially in countries with long transmission corridors like Brazil, China and India, there has been a renewed interest in this area [2], [3], [4].

In the U.K., the transfer capacity from Scotland to England needs to increase significantly to secure the growing demand in the south with the wind penetration in the north. Two sub-sea HVDC links, each rated at around 2 GW are planned along the east and west coasts [5] to add capacity and also enhance the stability limit of the existing Scottish-English inter-connector. The western link, which is currently under development is based on current source converter (CSC) technology with a planned completion date of 2015, while the one running along the east coast is likely to be of voltage source converter (VSC) technology [6], with an anticipated completion date of 2018.

Most of the work on HVDC control to damp oscillations, including [2], [3], [4], have primarily focused on HVDC networks based on CSC technology. A VSC HVDC link allows independent modulation of active power and reactive power (at both ends) and hence offers more flexibility than CSC where only the active power can be modulated. There is tremendous potential for VSC HVDC systems to contribute towards improvement in AC system dynamic performance as discussed in [7], [8], [9].

The challenge, however, is to coordinate the supplementary control action properly at the two ends of the link without the use of centralized control, which requires fast communication of control signals to remote actuator (converters) sites. Of course wide area measurement systems (WAMS) are needed to communicate phasor measurement units (PMU) signals to the control centers. A sequential loop-closure strategy for multiple flexible ac transmission systems (FACTS) whereby each control loop is designed independently was introduced in [10]. Such a sequential design does not take into account the presence of all the control inputs simultaneously, thus proper coordination and allocation of control effort among all available control inputs is not addressed in a systematic way.

In this work, coordinated supplementary control of the real and reactive power reference of the rectifier side VSC HVDC converter and the reactive power reference of the inverter side VSC HVDC converter is proposed. The idea is to ensure appropriate sharing of the overall control duty and thus lessen the burden on each. One way to achieve coordinated control is to design all the control loops simultaneously in a multi-variable framework. However, the resulting full multi-input, multi-output (MIMO) controller is difficult to implement in a decentralized (control center located at the actuator site) way as it requires all the feedback signals, some or all of which could be from remote locations, to be transmitted to each actuator location. Moreover, because of the cross-coupling between the control loops through the off-diagonal terms of the controller, the closed-loop performance could be potentially worse than open-loop in case of loss of one or more remote feedback signal(s). On the other hand, if the control structure is block-diagonal, the individual control loops are decoupled from each other which is not only simpler to implement in a decentralized way but also guarantees a minimum level of performance through the healthy control loops in the event of

Support from the EPSRC UK under grant EP/F037686 (Power Networks Research Academy) is gratefully acknowledged.

The authors are with the Control and Power Research group, Imperial College, London, United Kingdom.
e-mail:{*y.pipelzadeh08, b.chaudhuri, t.green*}*@imperial.ac.uk*

loss of one or more (but not all) remote feedback signals.

Of course, the controller is required to be robust for a range of operating conditions. A procedure based on H_∞ is discussed in [11] for tuning multiple FACTS devices. In [12], a dynamic output feedback for decentralized design using linear matrix inequality (LMIs) considering multiple operating conditions is illustrated. The controller order, however, is the same as the dimension of the open-loop plant for both these approaches which could be prohibitively large for practical implementation. An analytical design formulation using homotopy is introduced in [13], where a full MIMO controller can be deformed into a block diagonal structure resulting in a set of low order single-input, single-output (SISO) decentralized controllers. This approach was applied in controlling structural vibrations during large disturbances such as earthquakes [14].

In this paper, our main research question is: Can a set of decentralized, robust SISO controllers be designed for supplementary control at the two ends of a VSC HVDC link embedded within a power system such that the control action is coordinated and a minimum performance level is guaranteed in the event of loss of a remote feedback signal?.

To address this, first a MIMO controller is designed in LMI framework to achieve coordination amongst the modulation of active and reactive power at either end of the VSC HVDC link. An extension to the standard homotopy framework is proposed [13] such that a single block-diagonal decentralized controller is obtained from a set of full centralized controllers, individually designed to ensure specified closed-loop performance for a set of operating conditions. Thus both robustness and control coordination is achieved simultaneously in a decentralized framework without the need for fast communication of control signals to remote actuator (converters) sites. The terms *'decentralized'* and *'block-diagonal'* are used interchangeably throughout the rest of the paper.

II. Robust Decentralized Control: Homotopy Approach

The control design is formulated in two-stages. In the first stage, a centralized controller, G_C(s) is computed using methods reported in [12], [15], [16]. In the second stage, the controller matrices are deformed from full matrices defined by a centralized controller, as shown in Fig. 1(a) to block diagonal matrices which describes a decentralized control structure, G_D(s), as shown in Fig. 1(b).

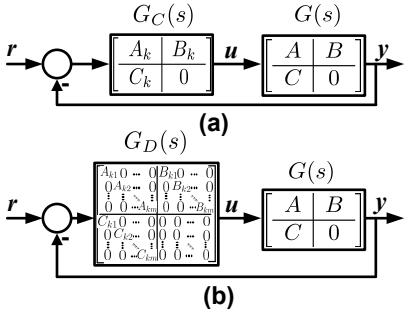

Fig. 1. Closed loop system with (a) full centralized controller and (b) block-diagonal decentralized controller.

A. Design of Centralized Damping Controller

Consider a linearized system model $G_i(s)$ expressed in state-space form as:

$$G_i(s) \triangleq \left[\begin{array}{c|c} A_i & B_i \\ \hline C_i & 0 \end{array}\right] \qquad (1)$$
$$A \in \Re^{n\times n},\ B \in \Re^{n\times m},\ C \in \Re^{m\times n}$$

Where i represents the i^{th} operating condition. The objective is to synthesize a full-order centralized linear output feedback controller $G_{C_i}(s)$ using [15], where:

$$G_{C_i}(s) \triangleq \left[\begin{array}{c|c} A_{k_i} & B_{k_i} \\ \hline C_{k_i} & 0 \end{array}\right] \qquad (2)$$
$$A_k \in \Re^{n\times n}, B_k \in \Re^{n\times m}, C_k \in \Re^{m\times n}$$

The closed loop system is synthesized by feedback connection of (1) & (2) represented by $\dot{\tilde{x}} = \tilde{A}_i\tilde{x}$.

where, $\dot{\tilde{x}} \in \Re^{2n}$ corresponds to the combined state vector of both the plant and the controller. The closed loop transfer function is given by $T(s) = \tilde{C}_i(sI - \tilde{A}_i)\tilde{B}_i + \tilde{D}_i$ with the closed loop system matrices $\tilde{A}_i, \tilde{B}_i, \tilde{C}_i, \tilde{D}_i$ given by:

$$\left[\begin{array}{c|c} \tilde{A}_i & \tilde{B}_i \\ \hline \tilde{C}_i & \tilde{D}_i \end{array}\right] = \left[\begin{array}{cc|c} A_i & B_iC_{k_i} & B_i \\ B_{k_i}C_i & A_{k_i} & 0 \\ \hline C_i & 0 & 0 \end{array}\right] \qquad (3)$$

Without any loss of generality, it can be assumed that the direct transmission term $\tilde{D}$ can be neglected as it does not influence the mode. The criterion of stabilizing system (1) by the centralized controller (2) is subject to finding $A_{k_i}, B_{k_i}, C_{k_i}$ and $\tilde{P}_i > 0$, subject to satisfying the inequality:

$$\tilde{A}_i\tilde{P}_i + \tilde{P}_i{\tilde{A}_i}^T < 0 \qquad (4)$$

However, satisfying the inequality in (4), will only guarantee stability. i.e. the poles located in the left half plane. In power system applications, its a requirement that power oscillations settle within 10 – 15 s [17]. This can be achieved if the closed-loop poles corresponding to the critical poles have a minimum damping ratio.

Minimum Damping Performance: A customary way to ensure satisfactory closed-loop transients is to place the closed-loop poles in a suitable region of the complex plane. This approach is referred to as regional pole-placements, where the closed-loop poles are assigned to specific locations in the complex plane. This is formulated in terms of LMI regions based on a 'conic sector' which is appropriate for power system damping control applications as it defines a minimum damping for the closed loop dominant inter-area modes[18].

The closed-loop system is guaranteed to have all its poles in the conic sector with apex at the origin and internal angle θ if and only if there exists a symmetric matrix $\tilde{P}_i > 0$ such that:

$$\begin{bmatrix} \sin\theta(\tilde{A}_i\tilde{P}_i + \tilde{P}_i{\tilde{A}_i}^T) & \cos\theta(\tilde{A}_i\tilde{P}_i - \tilde{P}_i{\tilde{A}_i}^T) \\ \cos\theta(\tilde{P}_i{\tilde{A}_i}^T - \tilde{A}_i\tilde{P}_i) & \sin\theta(\tilde{A}_i\tilde{P}_i + \tilde{P}_i{\tilde{A}_i}^T) \end{bmatrix} < 0 \qquad (5)$$

The inequality in (5) contains the product $\tilde{A}\tilde{P}$ which are functions of the controller parameters A_k, B_k, C_k and the controller parameters themselves are function of $\tilde{P}$. This leads to

$\tilde{A}\tilde{P}$ becoming non-linear in $\tilde{P}$. Following the practice outlined in [15], it is possible to linearize the problem through change of controller variables. The resulting centralized controller is obtained as $G_{c_i}(s) = C_{ki}(sI - A_{ki})^{-1}B_{ki}$. The damping ratio of all the poles lying inside the sector is guaranteed to have minimum damping ratio $\zeta = cos\vartheta$.

Remark 1.1: The order of the controllers synthesized using LMI based techniques are at least as high as the order of the linear system. Therefore, it is mandatory to simplify the system model, if possible, to ease the design procedure and avoid complexity in the final controller.

Remark 1.2: H_∞ performance objectives (see, eg. [15], [19]) could have been included as an additional constraint on the closed-loop system to provide a certain level of robustness with changing operating condition. The objective of the robust stabilization problem is to ensure stability under uncertainties in the system model. However, there may be uncertainties against which the controller is unable to ensure stability.

Remark 1.3: The formulation above is capable of obtaining a single centralized controller designed based on the i^{th} operating condition. Robustness for multiple operating points is necessary and is dealt with in the second design stage.

B. Deformation of Centralized to Decentralized Controller

In this stage, the concept of homotopy is applied to obtain a single block-diagonal controller from a single full controller [13]. An extension to this approach is then introduced, allowing a single block-diagonal controller to be reached from a set of centralized controllers, individually designed to ensure specified closed-loop performance from its respective operating condition.

Lets re-write $\tilde{A}_i$ from (3) as:

$$\tilde{A}_i \triangleq \underbrace{\left[\begin{array}{c|c} A_i & 0 \\ \hline 0 & 0 \end{array}\right]}_{\hat{\mathrm{A}}_\mathrm{i}} + \underbrace{\left[\begin{array}{c|c} 0 & B_i \\ \hline I & 0 \end{array}\right]}_{\hat{\mathrm{B}}_\mathrm{i}} \underbrace{\left[\begin{array}{c|c} A_{ki} & B_{ki} \\ \hline C_{ki} & 0 \end{array}\right]}_{\mathrm{G_{Ci}}} \underbrace{\left[\begin{array}{c|c} 0 & I \\ \hline C_i & 0 \end{array}\right]}_{\hat{\mathrm{C}}_\mathrm{i}} \tag{6}$$

by substituting (6) into (4) this problem is equivalent to the existence of $\tilde{P} \in \mathbf{SR}^{n\times n}$ such that:

$$\tilde{P}_i > 0,$$

$$F(G_{Ci}, \tilde{P}_i) = (\hat{A}_i + \hat{B}_i G_{Ci} \hat{C}_i)^T \tilde{P}_i + \tilde{P}_i (\hat{A}_i + \hat{B}_i G_{Ci} \hat{C}_i) \tag{7}$$

where,

F : A matrix variable as a function of G_C and $\tilde{P}$

$\boldsymbol{SR}$: A set of real stable controllers

Remark 2.1: A_k, B_k, C_k are 'full' matrices (defining G_C) which are computed using LMIs as reported in [15]. However, since the objective here is to impose decentralized (block-diagonal) structure on these matrices, this leads to a problem with bilinear matrix inequality (BMI).

Remark 2.2: The computational complexity for solving BMI problems is far greater than LMI problems since they are non-convex and can have multiple solutions.

Remark 2.3: A solution to such optimization problem with bilinear matrix inequality (BMI) constraints in (7), with both G_D and $\tilde{P}$ being unknowns, is not straightforward. To solve such BMI problem, the homotopy method is employed here to solve the BMI iteratively.

The conceptual idea is that at each stage, groups of variables are fixed alternately at the iterations to reduce the BMI to LMIs. In other words, the BMI constraints in (7) can be transformed into a set of LMI constraints by simply holding either G_C or $\tilde{P}$ constant at a time, such that only one variable needs to be solved at one time. The transformation into LMIs can then be solved very efficiently [13].

Lets consider a real number λ which gradually varies from $0 \rightarrow 1$, and lets introduce a homotopy path $H(G_{Di}, \tilde{P}_i, \lambda_i)$ from G_C to G_D such that:

$$H(G_{Di}, \tilde{P}_i, \lambda_i) = F\left((1-\lambda_i)\, G_{Ci} + \lambda_i G_{Di}, \tilde{P}_i\right) \tag{8}$$

where matrix variable H is a function of G_D, $\tilde{P}$ and λ.

Notice the term $(1-\lambda)G_C + \lambda G_D$ in (8), with $\lambda = 0$, the result is a full structure controller G_C (i.e. initial stage of the computation) and when $\lambda = 1$, it converges onto a decentralized structure G_D reflecting the desired final stage. The solution lies in the family of problems:

$$H(G_{D_i}, \tilde{P}_i, \lambda_i) < 0 \tag{9}$$

The computational algorithm to arrive at a *block-diagonal* structure from a *full-controller* structure is outlined below. The reader is referred to [13], [14] for further details.

Step 1: Given a plant model, $G(s)$ design a centralized controller, $G_C(s)$ using the method of [15].

Step 2: Define M as the total number of homotopy steps, set $M = 2^8$, an upper max $M_{max} = 2^{13}$, $\lambda_0 := 0$, $k := 0$ and $G_{D0} := 0$. Then compute a feasible solution of $\tilde{P}_0$ under the constraint $H(G_{D0}, \tilde{P}_0, \lambda_0) < 0$.

Step 3: Set $k := k + 1$, with incremental steps $\lambda_k := k/M$; compute solution of G_D under the constraint $H(G_D, \tilde{P}_{k-1}, \lambda_k) < 0$. If condition is not satisfied, go to Step 4. If satisfied, set $G_{Dk} := G_D$, and solve for $\tilde{P}$ under the constraint $H(G_{Dk}, \tilde{P}, \lambda_k) < 0$. If a feasible solution is reached, set $\tilde{P}_k := \tilde{P}$, and go to Step 6.

Step 4: Compute a solution of $\tilde{P}$ for $H(G_{D_{k-1}}, \tilde{P}, \lambda_k) < 0$. If condition is not satisfied, go to Step 5. If satisfied, set $\tilde{P}_k := \tilde{P}$ and solve for G_D under the constraint $H(G_D, \tilde{P}_k, \lambda_k) < 0$. If condition is feasible, set $G_{Dk} := G_D$ and go to Step 6; else go to Step 5.

Step 5: Set $M := 2M$ under the constraint $M \leq M_{max}$, and go to Step 2.

Step 6: If $k < M$, go to Step 3. Else, if $k = M$, a solution is reached with G_{Dk} of block-diagonal structure.

Remark 2.4: The feasibility of the resulting LMIs depend on the values assigned to the variables. An inappropriate assignment can result in an infeasible solution of the LMI problem even though its original BMI may be feasible.

To capture realistic sets of control design specifications for power system applications further objectives such as robustness with changing operating condition are considered in the design to guarantee satisfactory operational performance.

Simultaneous design for Robustness: Operating condition of a power system changes frequently. Hence, linearizing the power system for (say, l) operating conditions allows for the design of controllers that provide robustness across a range of operating conditions. The algorithm proposed in the previous section transforms a single centralized controller designed based on a particular operating condition into a decentralized controller. A generalization for l operating conditions that results in a single decentralized controller can be obtained by considering $i = 1, 2 \cdots l$, for equations (6-8).

To illustrate this, lets consider two centralized controllers G_{C1} and G_{C2}, designed based on power system models $(A_1, B_1, C_1, 0)$ and $(A_2, B_2, C_2, 0)$ respectively. Through two different homotopy paths $H(G_{D1}, \tilde{P}_1, \lambda_1)$ and $H(G_{D2}, \tilde{P}_2, \lambda_2)$, G_{D1} and G_{D2} are separately reached. By including a constraint of equating $G_{D1} = G_{D2}$, a single decentralized controller capable of stabilizing two operating conditions is obtained. The following system definitions defined below for equations (6-8) are used.

$$\left[\begin{array}{c|c} \mathcal{A} & \mathcal{B} \\ \hline \mathcal{C} & * \end{array}\right] = \left[\begin{array}{cc|cc} \hat{A}_1 & 0 & \hat{B}_1 & 0 \\ 0 & \hat{A}_2 & 0 & \hat{B}_2 \\ \hline \hat{C}_1 & 0 & * & * \\ 0 & \hat{C}_2 & * & * \end{array}\right]$$

$$\hat{A}_i \in \Re^{n\times n}, \hat{B}_i \in \Re^{n\times 1}, \hat{C}_i \in \Re^{1\times n},\ i = 1, 2 \tag{10}$$

$$\mathcal{P} = \left[\begin{array}{cc} \tilde{P}_1 & 0 \\ 0 & \tilde{P}_2 \end{array}\right] \lambda = \left[\begin{array}{cc} \lambda_1 & 0 \\ 0 & \lambda_2 \end{array}\right] \tag{11}$$

$$\mathcal{G}_C = \left[\begin{array}{cc} G_{C1} & G_{C2} \end{array}\right] \mathcal{G}_D = \left[\begin{array}{cc} G_{D1} & G_{D2} \end{array}\right] \tag{12}$$

The reason for selecting homotopy method over the usual iterative methods is that it has been observed that the domain of attraction of a solution point for iterative methods is usually much smaller than that for homotopy methods. However, due to the nature of the algorithm, non-convergence does not imply that a solution to the BMI problem does not exist. The drawbacks of this technique are that for systems of high order, the computational algorithm can become very time-consuming. Model reduction can be applied to reduce the computational burden and hence improve the convergence time.

The application of this approach for designing decentralized controllers for power systems is considered in the next section.

III. Case Study I: Four-Machine, Two-Area System

A. Test System Description

To start with, a case study was carried out on the well-known four-machine, two-area test system shown in Fig. 2. A point-to-point VSC based HVDC link is installed in parallel to the AC corridors between buses 7 and 9. The AC-DC system was modeled in DIgSILENT PowerFactory after verifying the AC part against the results in [20]. The loads are assumed to be a mix of constant current and constant impendence types (CC/CI). Here, all four generators were represented using the sub-transient model with a DC (IEEE-DC1A type) excitation system [21] and without power system stabilizers (PSS). The converters are rated at 224 MVA and the line ratings of the VSC HVDC link were adopted from those of the CSC HVDC system in [20].

Two different loading conditions are presented here. Under normal loading the power transfer through the AC tie-lines from West to East was approximately 400 MW. By adjusting the loads at buses 7 and 9, a heavy loading scenario with 600 MW tie-line flow was also simulated. Under both scenarios, the steady-state active power order for the rectifier was fixed at 200 MW. The reactive power order was set to maintain close to unity power factor at the terminal AC buses, 7 and 9.

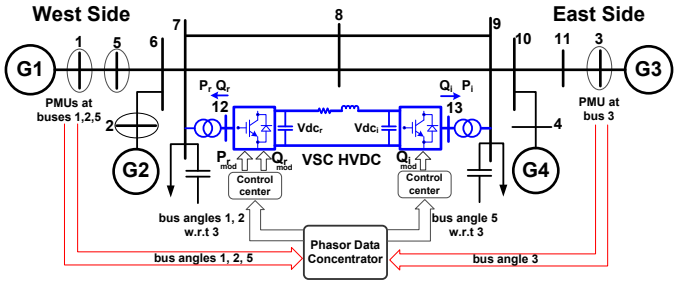

Fig. 2. Test system I: Four-machine, Two-area system with a VSC HVDC link (shown in blue). Secondary control loops with PMU signals are shown.

B. VSC HVDC Link Modeling

PWM was considered for the control of the VSC HVDC system and the converters were represented by their averaged model. The dc link was represented by a lumped parameter model. A decoupled current control strategy in the modified reference frame ($d'q'$) and standard PI controllers were used, see Fig. 3(a),(b). PLL locks the d'-axis to the AC voltage at the inverter PCC (E_{ac}) to ensure decoupled control [22].

1) Rectifier Control: The rectifier operates in $P-Q$ control mode with decoupled control strategy [22] as shown in Fig. 3(c). The reference values of the current components were derived as:

$$i_d^{'*} = \frac{2P_{rec}^*}{3E_{ac}}, i_q^{'*} = -\frac{2Q_{rec}^*}{3E_{ac}} \tag{13}$$

2) Inverter Control: The inverter operates in $V_{dc}-Q$ mode maintaining constant dc bus voltage and unity power factor on the point of common coupling, as shown in Fig. 3(d).

C. Control Loop Selection

All nodes were considered as potential sites for PMU feedback, such that time-synchronized phase angle measurements data is available at the control centers of the VSC HVDC.

For best feedback signals, residue analysis [20], [23] and relative gain array (RGA) were used to identify the most appropriate control-loops avoiding possible interactions [24].

RGA can be an additional tool to the residue analysis providing a systematic method for measuring two-way interactions between a determined input and output. It has been widely reported and commonly used in power system studies [25],[26],[27].

There are 4 possible control (modulation) inputs P_{rmod}, Q_{rmod}, V_{dcimod} and Q_{imod}, and 11 possible outputs (the phase

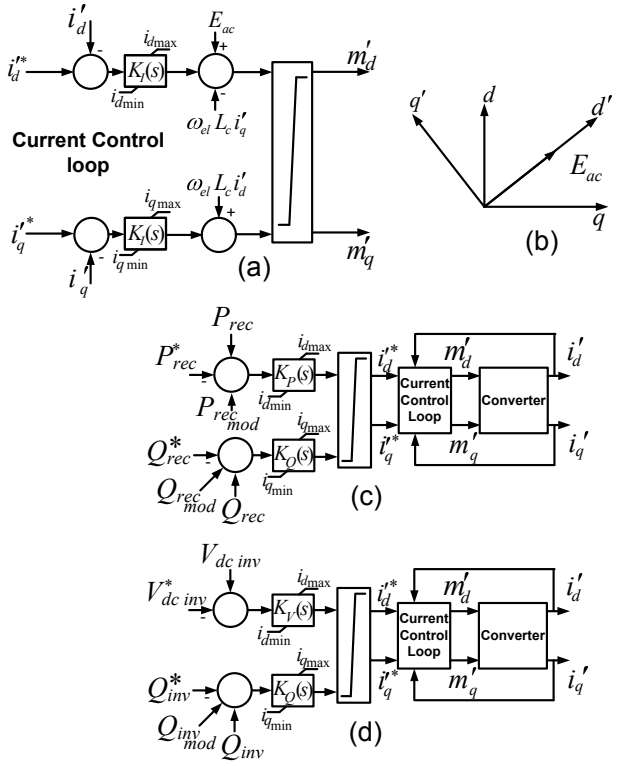

Fig. 3. (a) Inner current control (b) modified reference frame for decoupled control (c) rectifier control (d) Inverter control.

angles measured by the PMUs installed at 11 buses). Residues were calculated for all possible input-output combinations. The magnitudes and phase angles of the residues under normal loading condition are shown in Table I.

TABLE I
RESIDUES WITH MEASURED PHASE VOLTAGES ANGLES AT 11 BUSES AND 4 CONTROL INPUTS OF THE VSC HVDC UNDER NORMAL LOADING CONDITION

bus no.	P_{rmod}		Q_{rmod}		V_{dcimod}		Q_{imod}	
	mag	ang	mag	ang	mag	ang	mag	ang
1	**1.0**	-87	**0.64**	88	0.06	12	**0.67**	-99
2	**0.91**	-88	**0.59**	88	0.06	12	**0.61**	-99
4	0.17	-106	0.11	70	0.01	-5	0.11	-117
5	**0.95**	-88	**0.61**	88	0.06	12	**0.64**	-99
6	0.86	-88	0.55	88	0.05	12	0.57	-100
7	0.77	-88	0.50	87	0.05	11	0.52	-100
8	0.47	-91	0.30	84	0.03	8	0.32	-103
9	0.21	-102	0.13	74	0.01	-1	0.14	-114
10	0.18	-104	0.12	72	0.01	-3	0.13	-115
11	0.15	-108	0.10	67	0.01	-8	0.10	-120

The modulation of the DC link voltage, $V_{dc_{imod}}$, yields practical limitation as far secondary control action is concerned. Further, with V_{dcimod} having very small residue, P_{rmod}, Q_{rmod}, and Q_{imod} were considered for secondary control. Three measured outputs - phase angles at buses 1, 2 and 5 (marked in bold) - were chosen for reliability in order of descending residue magnitudes. RGA was used to form appropriate input-output pair among P_{rmod}, Q_{rmod}, and Q_{imod} and phase angles at buses 1,2 and 5. Any input-output pair with negative RGA element were discarded to avoid adverse interactions. Based on the RGA elements in Table II for normal loading condition, bus angle 5 was chosen for P_{rmod}, bus angle 2 for Q_{imod} and bus angle 1 for Q_{rmod}, all taken relative to the slack bus 3 to form a 3-input, 3-output decentralized control structure. The feedback signals are shown in red, see Fig. 2.

TABLE II
RGA FOR POSSIBLE INPUT-OUTPUT COMBINATIONS

bus no.	Normal Loading		
	P_{rmod}	Q_{rmod}	Q_{imod}
1	-10.93	**12.48**	-0.54
2	-24.84	11.76	**4.08**
5	**36.78**	-23.24	-12.53

D. Damping Controller Design

For control design, a linearized state-space model , see (1) of the test system is required, which cannot be directly obtained from DIgSILENT. Therefore, an identification routine was used to accurately estimate linearized models of the power system, capturing the critical dynamics in the frequency range of interest. Here, numerical algorithm for sub-space state-space system identification (N4SID) technique [28], [29] was used to derive linear models by measuring simulated outputs (i.e tie-line flow, bus phase angle of voltages) in response to injected pseudo random binary sequence (PRBS) signals [30] at the VSC HVDC reference control inputs.

A multi-variable centralized controller of similar size to the identified plant model (40^{th} order) was synthesized. A damping ratio ζ = 0.1 was specified to ensure the modes settle within 10 s. This is the initial design step; the second design stage deforms the full order controller into a low-order decentralized controller.

The power system model can be reduced if the aim of the arbitrary pole-placement for all the closed-loop poles is relaxed to closed-loop stability with special emphasis on a few critical poles. Incidentally, this is exactly what is required in damping controller design in power system applications, where damping ratios of a few critical electromechanical modes are of importance in the frequency range of interest, assuming that the others are stable. Thus, to lessen the computational burden and convergence time on the controller design stage, the plant and centralized controller are both reduced to 12^{th} order using balanced truncation technique [31], without losing much of the relevant information in the frequency range of interest $0.1 - 1.0\ Hz$. The frequency response of the closed-loop system with the decentralized controller was found to be appreciably similar to that with full centralized controllers. This gives the confidence that the properties of the centralized controller are retained when deforming into a decentralized controller. The structure of the closed-loop system is illustrated in Fig. 10(a). The location of each individual actuator is local to its respective HVDC converter station. The final decentralized controller is made up of 3 x SISO controllers whereby each channel consists of only one gain (K) and three first-order lead-lag blocks terms, besides a washout blocks $(T_w = 2.0s)$. The controller structure is shown in Fig. 4. The structure and order of the compensators in each channel are chosen to reflect those of a standard PSS structure [20].

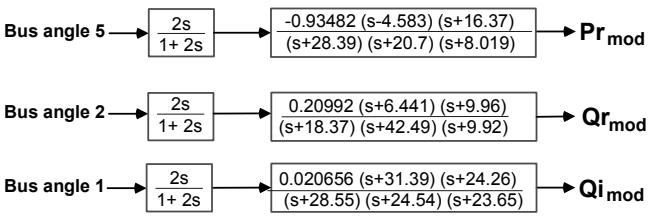

Fig. 4. Parameters of the PSSs for the VSC converters. Feedback signals taken relative to phase angle of bus 3.

E. Modal Analysis

The eigen-analysis of the study system was carried out for various scenarios. Table III shows the critical eigen values of the system under normal (400 MW tie-flow) and heavy loading (600 MW tie-flow) conditions.

TABLE III
DAMPING RATIOS AND FREQUENCIES OF CRITICAL MODES

Loading Condition	Base system		Centralized case		Decentralized case	
	$\zeta, \%$	f, Hz	$\zeta, \%$	f, Hz	$\zeta, \%$	f, Hz
Normal 400 MW	**1.5**	**0.568**	**8.1**	**0.556**	**11.3**	**0.547**
	8.4	1.064	8.3	1.065	8.2	1.065
	8.0	1.099	7.8	1.099	7.4	1.097
Heavy 600 MW	**0.7**	**0.540**	**10.0**	**0.513**	**12.5**	**0.516**
	8.6	1.060	8.6	1.061	8.5	1.059
	7.7	1.092	7.7	1.092	7.0	1.092

F. Non-linear Simulation

Time domain simulation were conducted in DIgSILENT PowerFactory for 20 s to further demonstrate performance robustness of the decentralized controller in the presence of system nonlinearities, including saturation. The dynamic performance of the system for different loading condition is shown in Figs 5 and 6.

1) Normal Loading condition: A three-phase solid self clearing fault at bus 8 for 83ms ($\approx$ 5 cycles) was created to trigger the inter-area oscillations – see Fig. 5 (a,b).

The dynamic response of the system is shown in Fig. 5(a) in terms of oscillations the tie-line power flow triggered by the above disturbance. Without any supplementary control the system response (in blue) is unacceptably oscillatory while with control, satisfactory response is achieved wherein the oscillations settle within 10-12 s. The relative angular separation of machine #1 from that of #3 is shown in subplot 5(b). Its evident from subplot 5(d) that active power modulation of the HVDC link mainly contributes towards stabilizing the oscillations with the reactive power modulation having minimal influence.

2) Heavy Loading condition: The dynamic behavior of the system following a 3-phase self clearing fault for 5 cycles on the inverter bus #9 of the AC system is illustrated in Fig. 6.

The power oscillation is seen to be light damped with non-linearities becoming noticeable, this is due to the increase in tie-line transfer, see blue trace in subplot 6(a). The modulated DC link power is demonstrated in subplot 6(c). As expected, the control effort demanded from the heavy loading condition

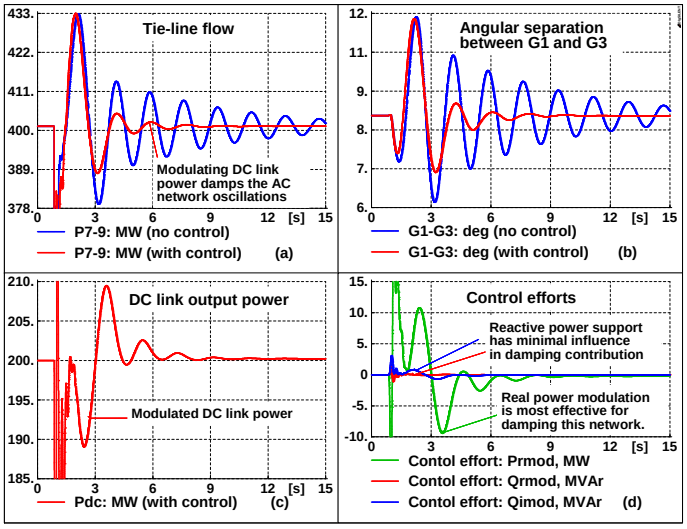

Fig. 5. Dynamic performance of the system under the normal loading condition. Plotted variables described below each subplot.

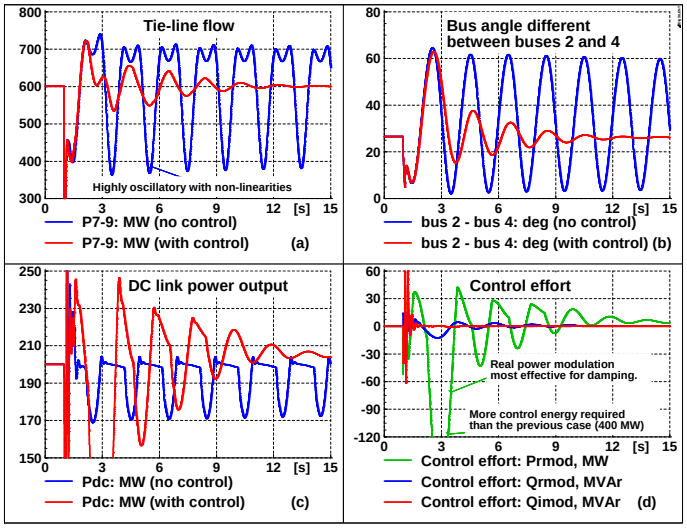

Fig. 6. Dynamic performance of the system for the heavy loading condition. Plotted variables described below each subplot.

is substantially higher relative to the normal loading condition. Since a fault is applied to the inverter side, a sharp increase in inverter side reactive power Q_{imod} is seen (red plot) in 6(d). Similar to the normal loading condition, active power modulation mainly contributes towards damping the oscillatory mode, with reactive power modulation becoming more evident under the heavy loading operating conditions – compare subplots 5(d) and 6(d).

IV. CASE STUDY II: FOURTEEN-MACHINE, FIVE-AREA SYSTEM

The proposed approach was validated on a more complex network, representing the Australian equivalent power system. The network shown in Fig.7 has been adopted as an IEEE benchmark for stability studies. A description of the system including machine, excitation system, and network parameters can be found in[32]. To provoke a more oscillatory behavior,

6 of the 14 PSSs (G1, G6, G8, G9, G11, G13) were placed out of service. The basis of the choice of which PSS to switch off was participation factor analysis. A VSC HVDC link is added between buses #102 and #217 (the region with the highest power transfer). The VSC HVDC is rated at 250 MVA, with line ratings of ± 150 kV. The steady state HVDC ratings are similar to those in Section III-A. Small signal analysis reveals three poorly damped inter-area modes.

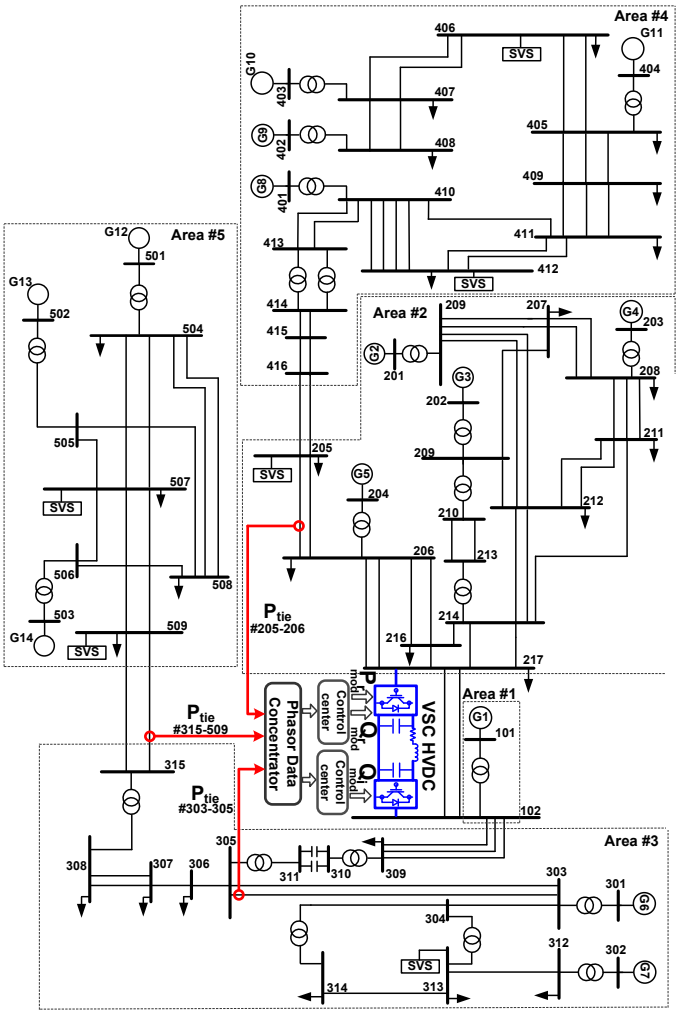

Fig. 7. Test system II: Fourteen-machine, Five-area system with a VSC HVDC link (in blue). Secondary control loops with remote feedback signals from PMUs are shown in red.

A. Damping Controller Design

The objective here is similar to that of Section III. The controller is designed to ensure that modal oscillations corresponding to each of the three critical inter-area modes settle within 10–15 s for a range of operating conditions. Linearized state-space models of 30^{th} order were found to accurately capture the dynamics of the power system. The plant and controller was further reduced to 21^{st} order with little relevant information lost in the frequency range of interest, as shown in Fig.9. Here, a base case and an outage case (tie-line #205-416 out of service) are reported. All nodes were considered as potential sites for PMU feedback with tie-line flows considered for remote feedback signal, as shown in Fig. 7. Modal residues reveal power flows in tie-lines #303-305, #315-509 and #205-206 as appropriate feedback signals for P_{rmod}, Q_{rmod}, and Q_{imod}, respectively. The synthesized decentralized controller is a 3 x SISO decentralized controller, whereby each input-output channel is of 7^{th} order, as shown in Fig. 8.

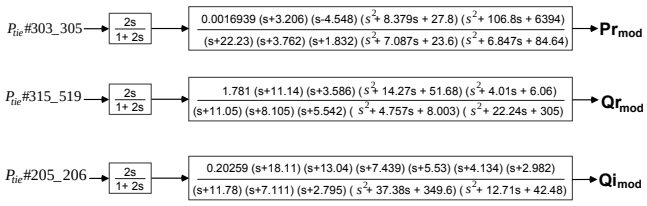

Fig. 8. Parameters of the PSSs for the VSC converters (real and reactive power modulation).

The frequency response of the closed loop system with centralized controller is comparable to that of the decentralized control, as shown in Fig.9.

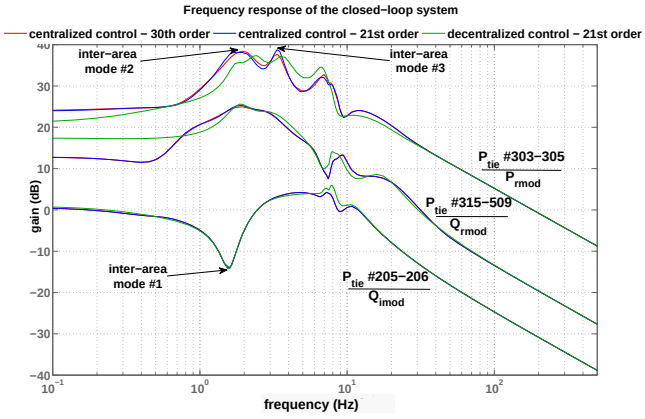

Fig. 9. Frequency response of the closed loop system (outage case) with centralized and decentralized control

From our experience, the feasibility of the algorithm depends on the initial centralized controller. The solver in MATLAB may result in numerical issues during the design of the decentralized control if models beyond the order of 30 are considered. We note that non-convergence of the algorithm for some centralized controllers does not generally indicate that the decentralized control problem has no solution. As discussed in Section III-D, model reduction techniques can be applied to reduce the plant size since only a few critical electromechanical modes in the frequency range (0.1 Hz – 2.0 Hz) are of interest. For the case studies considered here, reduced order plant and centralized controller models were considered for the design of the decentralized controller.

B. Eigen value Analysis

Eigen-analysis was performed for various operating conditions. Table IV shows the critical modes of the system under the base and outage scenarios. It's evident that the closed-loop system performance with decentralized control is slightly degraded from that of the centralized case. The next section

examines the closed loop performance of the decentralized control against the centralized case when a signal loss occurs.

TABLE IV
DAMPING RATIOS AND FREQUENCIES OF CRITICAL MODES

Operating condition	Base system		Centralized case		Decentralized case	
	$\zeta, \%$	f, Hz	$\zeta, \%$	f, Hz	$\zeta, \%$	f, Hz
Base	7.5	0.30	20.0	0.28	13.0	0.30
	8.2	0.35	11.5	0.35	12.8	0.38
	4.9	0.56	13.5	0.56	15.1	0.57
Outage	5.6	0.26	17.3	0.26	13.8	0.27
	10.2	0.34	17.1	0.33	13.3	0.37
	4.8	0.55	9.2	0.54	15.3	0.57

C. Signal loss

An important aspect is the effectiveness of the controllers in the event of a signal communication failure. Thus, a question arises; what is the impact on the closed loop system with (i) a centralized controller against that of (ii) a decentralized controller when a signal loss occurs? The conceptual idea is shown below in Fig. 10.

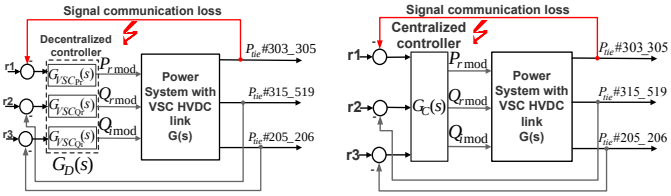

Fig. 10. Closed loop system with (a) decentralized control, (b) centralized control. Feedback signal loss shown in red.

Fig. 11 shows the frequency domain response of the closed loop system with a centralized control (upper subplot) and with a decentralized control (middle subplot) in the event of a communication signal loss from $P_{tie}\#303-305$. Interestingly, this signal loss mainly influences the dynamic response in mode #3. With the centralized case the closed-loop performance is worsened with respect to its open loop value as the mode has shifted further towards the imaginary axis. This is due to the cross-coupling between the control loops through the off-diagonal terms of the controller. However, with the decentralized case, the ability to damp this particular mode is degraded with respect to its nominal closed loop but the mode is shifted towards its open loop value. This is because the control structure is block-diagonal and individual control loops are decoupled from each other, which is not only easier to implement in a decentralized way, but also ensures a certain level of performance through the healthy control loops in the event of loss of one or more (but not all) remote feedback signals.

A standard PMU delay of 20 ms (corresponding to 50 Hz sampling) was considered and tested for possible performance deterioration up to a delay of 100 ms. However, as expected the low frequency (0.1 to 2 Hz) behavior was hardly affected by delays up to 100 ms. Of course, in the rare event of this delay going above 500 ms, the closed-loop response would start deteriorating. In such cases delays need to be considered

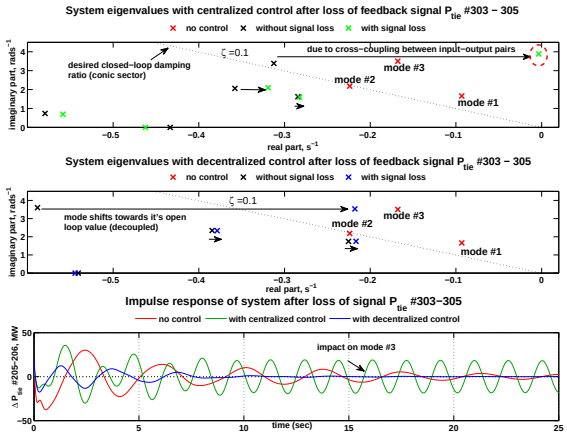

Fig. 11. Frequency and time-domain response of the system in the event of communication loss of signal $P_{tie}\#303-305$.

explicitly in the design stage although this aspect was not considered in this paper.

Fault tolerant design techniques could have been employed, rather than using a decoupled (family of SISO) structure to ensure a degree of robustness against sensor failure (or signal loss). However, the primary objective behind adopting a set of decoupled SISO controller here was ease of implementation with just one remote signal communicated to each actuator site while a MIMO controller (centralized) requires communication of all the remote feedback signals to every actuator location.

D. Non-Linear Simulation

To demonstrate the performance robustness of the damping controller across a range of operating conditions, a number of disturbances were simulated to trigger the multi-modal oscillation. Here, a fault on tie-line #205-416 for a duration of 100ms followed by opening of the circuit breakers, was considered. The objective is to demonstrate the ability of the decentralized controller to provide adequate damping across all the operating conditions that were considered in the design. It's evident from Fig.12(a-d) that the system response are stabilized within 10–15s.

The variation in the power output of the DC link is shown in Fig.12(d). Interestingly, a combination of both active and reactive power support are needed to effectively damp the AC oscillations, whereas in the previous case, active power control mainly contributed in power oscillation damping, see Fig.12(f). For bulk power systems, a mixture of active and reactive power are usually best suited for damping the oscillations; a finding that is in agreement with [7],[17],[33].

To understand the non-linear behavior in the reactive power modulation Q_{rmod}, shown in blue in Fig. 12(f), the variation in the HVDC actuator control parameters need to be analyzed. During the fault, the dc bus voltages at both ends increase sharply due to reduction of ac side power transfer. This is followed by oscillations in V_{dcr} due to the dc link dynamics, while V_{dci} is regulated to a constant value, see Fig 13(a,b). i_d and i_q are seen to have non-linearities 13(c-e), resulting from limiting hitting in the current control loop (see Fig. 3(a)).

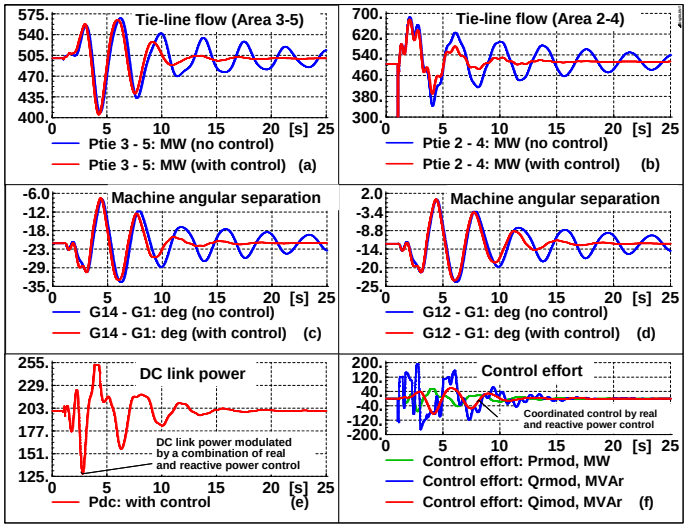

Fig. 12. Dynamic response with tie-line 205-416 outage. Plotted variables described below each subplot.

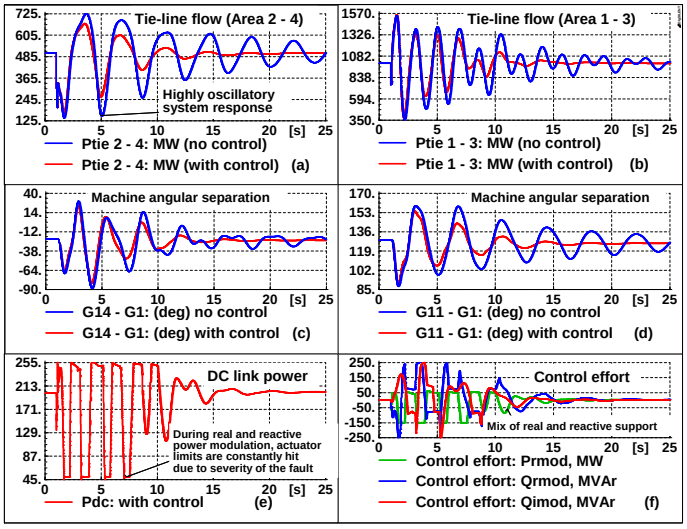

Fig. 14. Dynamic performance of the system following a 3 phase fault on bus #207, followed by tie-line 207-209 outage.

Consequently, the variation in active and reactive power will follow those of the currents – see relationship (13).

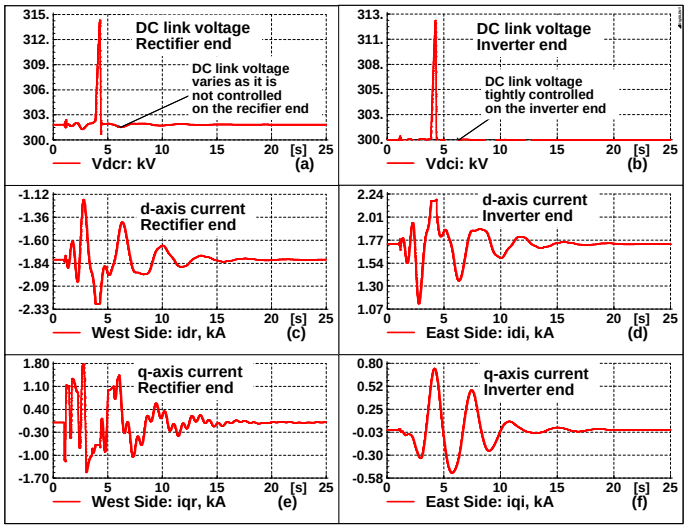

Fig. 13. HVDC actuator parameters dynamic response following tie-line 205-416 outage.

E. Robustness Validation

The robustness of the proposed decentralized control approach was verified for a range of operating conditions that were *not considered* in the design. Its assume that tie-line 205-406 is out of service due to maintenance and a fault is simulated on bus #207, followed by an outage of tie-line 207-209. The fault at this location is certainly a severe one as far as the transient stability is concerned, since this tie-line has one of the highest tie-flows. The dynamic response of the system following this $n-2$ contingency is shown in Fig. 14. As expected, the amplitude of the power oscillations is more than those in the previous case study, see subplots 14(a-d). The imposed limits on the current control result in a higher level of saturation in the modulated DC link, see subplot 14(e).

The fault scenario considered here is far more severe than the previous case with greater angular separation apparent – compare 12(c) with 14(c). Reactive power modulation becomes an important consideration in addition to real power under highly stressed conditions [17] demanding more reactive power support – compare 12(f) with 14(f). Control coordination ensures appropriate allocation/sharing of the overall duty amongst the active and reactive power as seen in subplot 14(f).

V. Conclusion

The application of homotopy is demonstrated for coordinated supplementary control of active and reactive power at both ends of a VSC HVDC link. The proposed approach achieves coordinated control with a decentralized control structure and thus, obviates the need for fast communication of control signals to remote control centres/ actuator (converter) site. Moreover, a minimum level of closed-loop performance is guaranteed in the event of loss of remote feedback signal(s) unlike a centralized approach where the performance could be worse due to cross-coupling between control loops. Further, an extension to the standard homotopy framework was proposed such that a single decentralized controller is synthesized from a set of centralized controllers designed for different operating conditions, thereby ensuring robustness and control coordination are simultaneously achieved.

References

[1] R. L. Cresap, W. A. Mittelstadt, D. N. Scott, and C. W. Taylor, "Operating experience with modulation of the pacific HVDC intertie," *IEEE Transactions on Power Apparatus and Systems*, vol. PAS-97, no. 4, pp. 1053–1059, 1978.

[2] M. Xiao-ming and Z. Yao, "Application of HVDC modulation in damping electromechanical oscillations," in *proceedings of IEEE Power Engineering Society General Meeting*, 2007, pp. 1–6.

[3] J. He, C. Lu, X. Wu, P. Li, and J. Wu, "Design and experiment of wide area HVDC supplementary damping controller considering time delay in china southern power grid," *IET Generation, Transmission & Distribution*, vol. 3, no. 1, pp. 17–25, 2009.

[4] P. Li, X. Wu, C. Lu, J. Shi, J. Hu, J. He, Y. Zhao, and A. Xu, "Implementation of CSG's wide-area damping control system: Overview and experience," in *proceedings of IEEE/PES PSCE Power Systems Conference and Exposition*, 2009, pp. 1–9.

[5] "ENSG: Our electricity transmission network: A vision for 2020," Feb 2012. [Online]. Available: www.decc.gov.uk/assets/decc/11/meeting-energy-demand/future-elec-network/4263-ensgFull.pdf

[6] J. Arrillaga, Y. H. Liu, and N. R. Watson, *Flexible power transmission: the HVDC options*. John Wiley, 2007.

[7] L. Zhang, L. Harnefors, and P. Rey, "Power system reliability and transfer capability improvement by VSC-HVDC," in *proceedings of Cigre Regional Meeting 20007*, 2007.

[8] H. F. Latorre, M. Ghandhari, and L. Soder, "Use of local and remote information in POD control of a VSC-HVDC," in *proceedings of PowerTech, 2009 IEEE Bucharest*, 2009, pp. 1–6.

[9] R. Si-Ye, L. Guo-Jie, and S. Yuan-Zhang, "Damping of power swing by the control of VSC-HVDC," in *proceedings of IPEC 2007 International Power Engineering Conference*, 2007, pp. 614–618.

[10] A. Messina, O. Begovich, J. López, and E. Reyes, "Design of multiple FACTS controllers for damping inter-area oscillations: a decentralised control approach," *International Journal of Electrical Power & Energy Systems*, vol. 26, no. 1, pp. 19–29, 2004.

[11] G. Taranto, J. Shiau, J. Chow, and H. Othman, "Robust decentralised design for multiple FACTS damping controllers," in *Generation, Transmission and Distribution,IET*, vol. 144, no. 1. IET, 2002, pp. 61–67.

[12] R. Ramos, L. Alberto, and N. Bretas, "A new methodology for the coordinated design of robust decentralized power system damping controllers," *IEEE Transactions on Power Systems*, vol. 19, no. 1, pp. 444–454, 2004.

[13] G. Zhai, M. Ikeda, and Y. Fujisaki, "Decentralized H [infinity] controller design: a matrix inequality approach using a homotopy method," *Automatica*, vol. 37, no. 4, pp. 565–572, 2001.

[14] Y. Wang, "Time-delayed dynamic output feedback H controller design for civil structures: a decentralized approach through homotopic transformation," *Structural Control and Health Monitoring*, 2009.

[15] M. Chilali and P. Gahinet, "Hinfinity design with pole placement constraints: an lmi approach," *IEEE Transactions on Automatic Control*, vol. 41, no. 3, pp. 358 –367, Mar. 1996.

[16] B. Chaudhuri and B. Pal, "Robust damping of multiple swing modes employing global stabilizing signals with a TCSC," *IEEE Transactions on Power Systems*, vol. 19, no. 1, pp. 499–506, 2004.

[17] J. Paserba *et al.*, "Analysis and control of power system oscillation," *CIGRE special publication*, vol. 38, no. 07, 1996.

[18] R. Majumder, B. Pal, C. Dufour, and P. Korba, "Design and real-time implementation of robust FACTS controller for damping inter-area oscillation," *IEEE Transactions on Power Systems*, vol. 21, no. 2, pp. 809–816, 2006.

[19] B. Chaudhuri and B. Pal, "Robust damping of multiple swing modes employing global stabilizing signals with a TCSC," *IEEE Transactions on Power Systems*, vol. 19, no. 1, pp. 499–506, 2004.

[20] P. Kundur, *Power system stability and control*, ser. The EPRI power system engineering series. New York; London: McGraw-Hill, 1994.

[21] "IEEE std 421.5 - 2005, IEEE recommended practice for excitation system models for power system stability studies," pp. 1–85, 2006.

[22] C. Schauder and H. Mehta, "Vector analysis and control of advanced static var compensators," *IEE Proceedings on Generation, Transmission and Distribution*, vol. 140, no. 4, pp. 299–306, 1993.

[23] S. Ray, B. Chaudhuri, and R. Majumder, "Appropriate signal selection for damping multi-modal oscillations using low order controllers," in *Power and Energy Society General Meeting-Conversion and Delivery of Electrical Energy in the 21st Century, 2008*. IEEE, 2008, pp. 1–7.

[24] S. Skogestad and I. Postlethwaite, *Multivariable feedback control: analysis and design*. Chichester: Wiley, 1996.

[25] L. Zhang, P. X. Zhang, H. F. Wang, Z. Chen, W. Du, Y. J. Cao, and S. J. Chen, "Interaction assessment of FACTS control by RGA for the effective design of FACTS damping controllers," *IEE Proceedings Generation, Transmission and Distribution,*, vol. 153, no. 5, pp. 610–616, 2006.

[26] W. Juanjuan, F. Chuang, and Z. Yao, "Design of wams-based multiple hvdc damping control system," *IEEE Transactions on Smart Grid*, vol. 2, no. 2, pp. 363–374, 2011.

[27] J. Milanovic and A. Duque, "Identification of electromechanical modes and placement of psss using relative gain array," *IEEE Transactions on Power Systems*, vol. 19, no. 1, pp. 410–417, 2004.

[28] P. van Overschee, *Subspace identification for linear systems : theory, implementation, applications*. Boston: Kluwer Academic, 1996.

[29] I. Kamwa, G. Trudel, and L. Gerin-Lajoie, "Low-order black-box models for control system design in large power systems," *IEEE Transactions on Power Systems*, vol. 11, no. 1, pp. 303–311, 1996.

[30] P. E. Wellstead and M. B. Zarrop, *Self-tuning Systems. Control and Signal Processing*. John Wiley & Sons, 1991.

[31] S. Skogestad, I. Postlethwaite, and I. NetLibrary, *Multivariable feedback control: analysis and design*. Wiley New York, 1996.

[32] M. Gibbard and D. Vowles, "Simplified 14-generator model of se australian power system," http://www.eleceng.adelaide.edu.au/groups/PCON/PowerSystems/IEEE/, 2008.

[33] T. Smed and G. Andersson, "Utilizing HVDC to damp power oscillations," *IEEE Transactions on Power Delivery*, vol. 8, no. 2, pp. 620–627, 1993.

Yousef Pipelzadeh (S'09) received his MEng in Communications Systems Engineering (with 1st class honors) in 2007. He then joined Wesley Clover International Corporation, Kanata, Ottawa until 2008. He is currently pursuing a Ph.D degree from Imperial College London, U.K. He is an active member of CIGRÉ and the Institution of Engineering and Technology (IET). His research interests are in the areas of power system dynamics and stability, HVDC transmission, and renewable energy systems.

Balarko Chaudhuri (M'06 - SM'11) received his PhD from Imperial College London in 2005. He worked with General Electric Global Research for a year before coming back to Imperial College as a post-doctoral research associate in 2006. He is presently a senior lecturer in the department of Electrical and Electronic Engineering at Imperial College London. His research interests are in the areas of power system dynamics and stability, FACTS/HVDC, robust control and renewable energy.

Tim C. Green (M'89-SM'02) received the B.Sc. (Eng.) degree from Imperial College London, London,U.K., in 1986, and the Ph.D. degree in electrical engineering from Heriot-Watt University, Riccarton, U.K., in 1990. Since 1994, he has been with the Imperial College, and is currently a Professor of electrical power engineering and Deputy Head of the Control & Power Research Group. He has held several U.K. government research grants and pursued industrially funded research with ABB, EDF Energy, and National Grid. He leads the Supergen FlexNet consortium of eight U.K. universities researching the future of electrical networks and the Aura-NMS consortium of seven universities developing active network management techniques. His teaching covers electrical power and machines, power electronics, drive systems and modeling, and control of electrical systems. His current research interests include the role of power electronics in future power systems, smart grids, the assessment and integration of renewable energy sources into electrical networks, supply quality improvement with distributed generation, the control of flexible ac transmission systems, and power electronics for microelectromechanical systems (MEMS) microgenerators. He is the author or coauthor of more than 55 published journal papers and more than 160 conference papers. Dr. Green is member of the Institution of Engineering and Technology (IET).